

Critical Relaxation and Critical Exponents ¹

H.J. Luo² and B. Zheng

Universität – GH Siegen, D – 57068 Siegen, Germany

Abstract

Dynamic relaxation of the XY model and fully frustrated XY model quenched from an initial ordered state to the critical temperature or below is investigated with Monte Carlo methods. Universal power law scaling behaviour is observed. The dynamic critical exponent z and the static exponent η are extracted from the time-dependent Binder cumulant and magnetization. The results are competitive to those measured with traditional methods.

PACS: 64.60.Ht, 75.10.Hk, 02.70.Lq, 82.20.Mj

¹Work supported in part by the Deutsche Forschungsgemeinschaft; DFG Schu 95/9-1

²On leave of absence from Sichua Union University, Chengdu, P.R. China

Much progress has recently been achieved in critical dynamics. For a critical relaxation process starting from a disordered state, it was recently argued by Janssen, Schaub and Schmittmann [1] with renormalization group methods that there exists universal scaling behaviour even *at macroscopic early times*, which set in right after a microscopic time scale t_{mic} . Important is that extra critical exponents should be introduced to describe the dependence of the scaling behaviour on the initial conditions [1, 2], or to characterize the scaling behaviour of special dynamic observables [3, 4, 5]. The critical exponent θ governing the initial increase of the magnetization and the exponent θ_1 characterizing the power law decay of the global persistence probability have numerically been determined to a satisfactory level for the Ising and the Potts model [6, 7, 8].

The short-time dynamic scaling is found to be quite general, for example, for the dynamics beyond model A [9], at tricritical point [10] and in surface critical phenomena [11] as well as with even more arbitrary initial conditions [12, 13, 14]. The investigation of the universal behaviour of the short-time dynamics not only enlarges the fundamental knowledge on critical phenomena but also, more interestingly, provides possible new ways to determine all the dynamic exponents as well as the static exponents. Especially, it has been demonstrated with the two-dimensional Ising model and Potts model that the extraction of the exponents from the power law behaviour of the observables at the beginning of the time evolution is rather efficient [15, 7, 13, 16]. Since our measurements do not enter the long-time regime of the dynamic evolution, the method may be free of critical slowing down. Therefore, it is interesting and important to investigate its application to complex systems where critical slowing down is more severe.

The two-dimensional XY model and fully frustrated XY model (FFXY) are two typical examples where numerical simulations are hampered by the severe critical slowing down. The dynamic relaxation of these two models starting from *a disordered state* with a small magnetization has been investigated with Monte Carlo methods [6, 17]. Critical initial increase of the magnetization is observed and the critical exponent θ is determined. However, as it is pointed out in the cases of the Ising model, the Potts model and the clock model [13, 18, 16], the determination of the static exponent η and the dynamic exponent z from this process is not the best choice. Sometimes the measurements of the auto-correlation and/or the second moment is not so easy. In comparison to this, the dynamic process starting from *an ordered state* shows its advantages for the measurements of the critical exponents [13, 19, 20].

In this letter, we numerically study the critical relaxation of the two dimensional XY and FFXY model starting from *an ordered state* and meanwhile determine the dynamic exponent z and the static exponent η from the time-dependent Binder cumulant and magnetization. Our results confirm the short-time dynamics scaling and show the dynamic measurement of the critical exponents is competitive with the traditional methods in equilibrium.

The XY model and FFXY model in two dimensions can be defined by the

Hamiltonian

$$H = K \sum_{\langle ij \rangle} f_{ij} \vec{S}_i \cdot \vec{S}_j, \quad (1)$$

where $\vec{S}_i = (S_{i,x}, S_{i,y})$ is a planar unit vector at site i and the sum is over the nearest neighbours. In our notation the inverse temperature has been absorbed in the coupling K . Here f_{ij} take the values $+1$ or -1 , depending on the models. For the XY model, $f_{ij} = 1$ on all links. A simple realization of the FFXY model is by taking $f_{ij} = -1$ on half of the vertical links (negative links) and others are $+1$ (positive links). This is shown in Fig. 1. The links marked by dotted lines represent the negative links.

Let us first concentrate our attention on the XY model. It is known that the XY model undergoes a Kosterlitz-Thouless phase transition at a certain critical temperature [21, 22]. This critical temperature is numerically known to be around $T_c = 1/K_c = 0.90$ [23]. Below the critical temperature, no real long range order emerges. The system remains critical in the sense that the spatial correlation length is divergent, therefore, an universal dynamic scaling form is expected in the whole time regime below the critical temperature. For example, for the k -th moment of the magnetization the scaling form is

$$M^{(k)}(t) = b^{-k\eta/2} M^{(k)}(b^{-z} t). \quad (2)$$

Taking $b = t^{1/z}$, one immediately obtain the power law behaviour for the magnetization $M(t) \equiv M^{(1)}(t)$

$$M(t) \sim t^{-\eta/2z}. \quad (3)$$

Here $M(t)$ can be any components of the vector magnetization defined as

$$\vec{M}(t) = \frac{1}{L^2} \sum_i \vec{S}_i \quad (4)$$

with L being the lattice size.

To determine z *independently*, we introduce a *time-dependent* Binder cumulant $U(t, L) = M^{(2)}/M^2 - 1$. Simple finite size scaling analysis shows

$$U(t, L) \sim t^{d/z}. \quad (5)$$

To simulate the dynamic relaxation, we take the initial state to be an ordered state, i.e. $\vec{S}_i = (S_{i,x}, S_{i,y}) = (1, 0)$ for all spins. Then the system is suddenly released to a dynamic evolution of model A [24] at the critical temperature or below. In this paper the Metropolis algorithm is mainly adopted, while some simulations are also carried out with the heat-bath algorithm to confirm universality. We stop update at the Monte Carlo time step $t = 750$ and then repeat the procedure. Average is taken over different random numbers. The total samples are 6 000 for the lattice size $L = 64$ and 32, while 4 500 for $L = 128$. Errors are estimated by dividing the samples into three groups.

In Fig. 2, the time evolution of the magnetization at the critical temperature $T_c = 1/K_c = 0.90$ [23] with both the Metropolis and the heat-bath algorithm is displayed for different lattice sizes. $M(t)$ is the x component of the magnetization $\vec{M}(t)$. The y component of the magnetization $\vec{M}(t)$ remains zero since the initial value is zero. The upper branch of the curves is the magnetization for the Metropolis algorithm while the lower one is that for the heat-bath algorithm. Dotted lines, solid lines and circles correspond to the lattice size $L = 32, 64$ and 128 . At the very beginning of the time evolution, the curves for the Metropolis and the heat-bath algorithm show quite different behaviour. After a certain time period, however, universal power law behaviour indeed emerges for both algorithms when the lattice size is sufficiently big. For the Metropolis algorithm, the curves for $L = 64$ and 128 overlap completely up to the time $t = 750$. The finite size effect for $L = 64$ is already negligibly small. In contrast to this, for the heat-bath algorithm at around $t = 300 - 400$ the curve for $L = 64$ starts bending down and shows significant finite size effect. This fact implies that the time scale of the heat-bath algorithm is large than that of the Metropolis algorithm. In other words, the time evolution with the heat-bath algorithm is faster. This can also be seen from the microscopic time scale t_{mic} , after which universal behaviour appears. For the heat-bath algorithm $t_{mic} \sim 20$, while for the Metropolis algorithm $t_{mic} \sim 80$. Actually, the curve for the Metropolis algorithm with $L = 32$ looks like that for the heat-bath algorithm with $L = 64$. Therefore the time scale for the heat-bath algorithm is roughly a factor of four larger.

	<i>Metropolis</i>		<i>Heatbath</i>	
L	64	128	64	128
$\eta/2z$.0622(05)	.0621(04)	.0637(13)	.0621(04)

Table 1: The exponent $\eta/2z$ measured with different lattice sizes and algorithms for the XY model.

T	0.90	0.86	0.80	0.70
z	1.96(4)	1.98(4)	1.94(2)	1.98(4)
η	.244(5)	.212(4)	.178(2)	.143(3)

Table 2: The exponent z and η measured for different temperatures with the Metropolis algorithm for the XY model. The lattice size is $L = 64$.

In the numerical simulations of the short-time dynamics, is the heat-bath algorithm more efficient or the Metropolis algorithm? The advantage for the heat-bath algorithm is that the microscopic time scale t_{mic} is really small and

there is clean universal scaling behaviour in the very early time. However, the heat-bath algorithm is in general more time consuming. In Table 1, the measured exponent $\eta/2z$ for both algorithms are listed. For the heat-bath algorithm, the measurements are carried out in a time interval [50, 300] while for the Metropolis algorithm in a time interval [200, 750]. In the numerical simulations the update to $t = 300$ for the heat-bath algorithm and $t = 750$ for the Metropolis algorithm need similar computer times. For the lattice size $L = 128$, both algorithms give the same results with the same quality. However, for the lattice size $L = 64$ the result for the heat-bath algorithm is much worse. The Metropolis algorithm shows its advantage in relatively small lattice.

From the power law decay of the magnetization, one can only obtain the combination $\eta/2z$ of the exponents. In order to determine the exponent z independently, we measure the time-dependent Binder cumulant $U(t, L)$. In Fig. 3, the cumulant $U(t, L)$ at the critical temperature with the Metropolis algorithm is displayed for lattice size $L = 64$ and 128. The measured exponent z is $z = 1.96(4)$ and $1.98(6)$ for the lattice size $L = 64$ and 128 respectively. We see again that the finite size effect for $L = 64$ is already negligibly small. The simulations with the heat-bath algorithm give similar results.

Compared with the dynamic process starting from a disordered state, the determination of the critical exponents from the dynamic relaxation from the ordered state is more efficient. The lowest two of non-zero moments in latter case are $M^{(1)}$ and $M^{(2)}$ in contrast to $M^{(2)}$ and $M^{(4)}$ in the former case. The values of $M^{(1)}(t)$ up to $t = 750$ shown in Fig. 2 is still rather big and therefore the fluctuations are small. The measurement of the cumulant constructed from $M^{(1)}$ and $M^{(2)}$ is also easier than that constructed from $M^{(2)}$ and $M^{(4)}$ in the former case.

Below the critical temperature, the XY model remains critical and similar scaling is expected. In Fig. 4, the time evolution of the magnetization at different temperatures with the Metropolis algorithm is displayed for lattice size $L = 64$. All values for the exponent z and η measured with the Metropolis algorithm and lattice size $L = 64$ are given in Table 2. With respect to the temperature the exponent z is rather clearly a constant very near $z = 2$. This is consistent with the theoretical prediction for the growth law in phase ordering [25]. For the static exponent η , the results are in very good agreement with those measured in equilibrium. In Ref [23], for example, large scale Monte Carlo simulations have been performed and it was reported that the static exponent $\eta = 0.238$ and 0.146 for the temperature $T = 0.90$ and 0.70 respectively. The agreement to the values in Table 2 is remarkable but our values of η show slightly more decreasing as the temperature decreases. The effort in our dynamic measurements is really not much. Especially we need not very big lattice in the numerical simulations of the short-time dynamics. With the statistics of 6 000 for a updating time $t = 300$ or $t = 750$, the errors are already at least comparable with those given in [23]. Besides the static exponent η , we also obtain the dynamic exponent z , the

measurement of which is very difficult with traditional methods. Further, if the static exponent η is known, we can get even more rigorous values for the dynamic exponent z from the power law decay of the magnetization $M(t)$ than that from the cumulant given in Table 2.

T	0.446	0.440	0.400	0.350	0.300
z	1.89(5)	1.93(4)	1.95(3)	1.99(7)	1.97(3)
η	.275(8)	.243(4)	.140(2)	.107(1)	.086(2)

Table 3: The exponent z and η measured for different temperatures with the Metropolis algorithm for the FFXY model. The lattice size is $L = 64$.

Encouraged by the success in the XY model, we have also performed similar simulations for the FFXY model. In equilibrium, due to the frustration of the couplings the numerical simulation of FFXY model is even more difficult than that for the XY model. The Kosteritz-Thouless critical temperature T_c is reported to be $T_c = 0.446$ [26, 27, 28] or $T_c = 0.440$ [29]. In the numerical simulations of the short-time dynamics, we take the initial ordered state as the ground state shown in Fig. 1. We measure the projection of the vector magnetization $\vec{M}(t)$ in the initial direction and denote it also as $M(t)$. From $M(t)$ and the second moment of $\vec{M}(t)$ we construct the Binder cumulant. In Fig. 5, the time-dependent Binder cumulant for the lattice size $L = 64$ with different temperatures is plotted in double-log scale. It is clear that nice power law behaviour appears for all the temperatures after a microscopic time scale $t_{mic} \sim 100$. The figure for the magnetization $M(t)$ looks similar as Fig. 4. All the measured exponents z and η for the lattice size $L = 64$ and with different temperatures are given in Table 3. The statistics is the same as for the XY model. From the errors in Table 2 and 3, we do not feel the simulations for the FFXY model is more difficult than those for the XY model. In Table 3, we see that the values for the dynamic exponent z are consistent with those for the XY model. For the static exponent η , our values are slightly bigger than those reported in Table V of Ref. [27]. However, the finite size effect of the results in Ref. [27] is still rather visible. For example, at the temperature $T = 0.440$ from the lattice size $L = 64$ to 96 the value of η changes from $\eta = 0.1666$ to 0.1955. One easily expects that for larger lattices the final value of η may reach ours $\eta = 0.243(4)$. In contrast to this, the finite size effect of our results is already negligible small.

Finally we would like to mention that our measured value for the dynamic exponent z at the temperature $T = 0.446$ is $z = 1.89(5)$. This is somehow smaller than that for other temperatures below $T = 0.446$. Further, the measured value $\eta = 0.275(8)$ for the exponent η at this temperature is also apparently above the theoretical prediction $\eta = 0.25$ at the critical temperature T_c . Therefore our results suggest that the critical temperature is near $T = 0.440$ rather than

0.446. The measured value $\eta = 0.243(4)$ at $T = 0.440$ is very close to the value $\eta = 0.244(5)$ for the XY model at the measured critical temperature $T_c = 0.90$ and the theoretical prediction $\eta = 0.25$ for the Kosterlitz-Thouless phase transition.

In conclusions, we have numerically investigated the universal short-time behaviour of the critical relaxation of the XY model and fully frustrated XY model starting from an ordered state. We show that even for more complex systems as the XY model and the FFXY model, we can obtain rigorously the dynamic exponent z and the static exponent from the short-time dynamics. Our measurements are not hampered by critical slowing down.

Acknowledgement: One of the authors (H.J. Luo) would like to thank the Heinrich Hertz Stiftung for a fellowship.

References

- [1] H. K. Janssen, B. Schaub and B. Schmittmann, Z. Phys. **B 73** (1989) 539.
- [2] D. A. Huse, Phys. Rev. **B 40** (1989) 304.
- [3] S.N. Majumdar, C. Sire, A.J. Bray and S. Cornell, Phys. Rev. Lett. **77** (1996) 2867.
- [4] L. Schülke and B. Zheng, Phys. Lett. **A 233** (1997) 93.
- [5] K. Oerding, S.J. Cornell and A.J. Bray, Phys. Rev. **E56** (1997) R25.
- [6] K. Okano, L. Schülke, K. Yamagishi and B. Zheng, J. Phys. A: Math. Gen. **30** (1997) 4527.
- [7] P. Grassberger, Physica **A 214** (1995) 547.
- [8] Z.B. Li, U. Ritschel and B. Zheng, J. Phys. A: Math. Gen. **27** (1994) L837.
- [9] K. Oerding and H. K. Janssen, J. Phys. A: Math. Gen. **26** (1993) 3369,5295.
- [10] K. Oerding and H. K. Janssen, J. Phys. A: Math. Gen. **27** (1994) 715.
- [11] U. Ritschel and P. Czerner, Phys. Rev. Lett. **75** (1995) 3882.
- [12] Z.B. Li, L. Schülke and B. Zheng, Phys. Rev. Lett. **74** (1995) 3396.
- [13] L. Schülke and B. Zheng, Phys. Lett. **A 215** (1996) 81.
- [14] B. Zheng, Phys. Rev. Lett. **77** (1996) 679.
- [15] L. Schülke and B. Zheng, Phys. Lett. **A 204** (1995) 295.
- [16] K. Okano, L. Schülke, K. Yamagishi and B. Zheng, Nucl. Phys. **B 485** (1997) 727.
- [17] H.J. Luo, L. Schülke and B. Zheng, Phys. Rev. **E57** (1998) 1327.
- [18] P. Czerner and U. Ritschel, Phys. Rev. **E 53** (1996) 3333.
- [19] D. Stauffer and R. Knecht, Int. J. Mod. Phys. **C7** (1996) 893.

- [20] D. Stauffer, *Physica* **A 186** (1992) 197.
- [21] J.M. Kosterlitz and D.J. Thouless, *J. Phys.* **C 6** (1973) 1181.
- [22] J. Kosterlitz, *J. Phys.* **C 7** (1974) 1046.
- [23] R. Gupta and C.F. Bailie, *Phys. Rev.* **B 45** (1992) 2883.
- [24] P.C. Hohenberg and B.I. Halperin, *Rev. Mod. Phys.* **49** (1977) 435.
- [25] A. D. Rutenberg and A. J. Bray, *Phys. Rev.* **E 51** (1995) R1641.
- [26] G. Ramirez-Santiago and J. José, *Phys. Rev. Lett.* **68** (1992) 1224.
- [27] G. Ramirez-Santiago and J.V. José, *Phys. Rev.* **B49** (1994) 9567.
- [28] P. Olsson, *Phys. Rev. Lett.* **75** (1995) 2758.
- [29] S. Lee and K. Lee, *Phys. Rev.* **B 49** (1994) 15184.

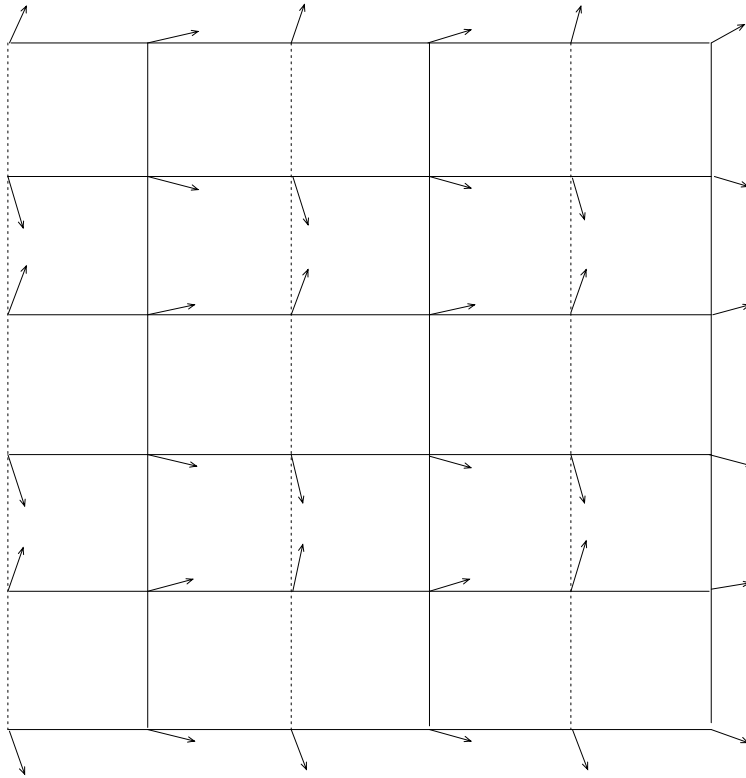


Figure 1: A simple realization of the FFXY model and one of the ground states. The dotted vertical lines represent the negative links with $f_{ij} = -1$.

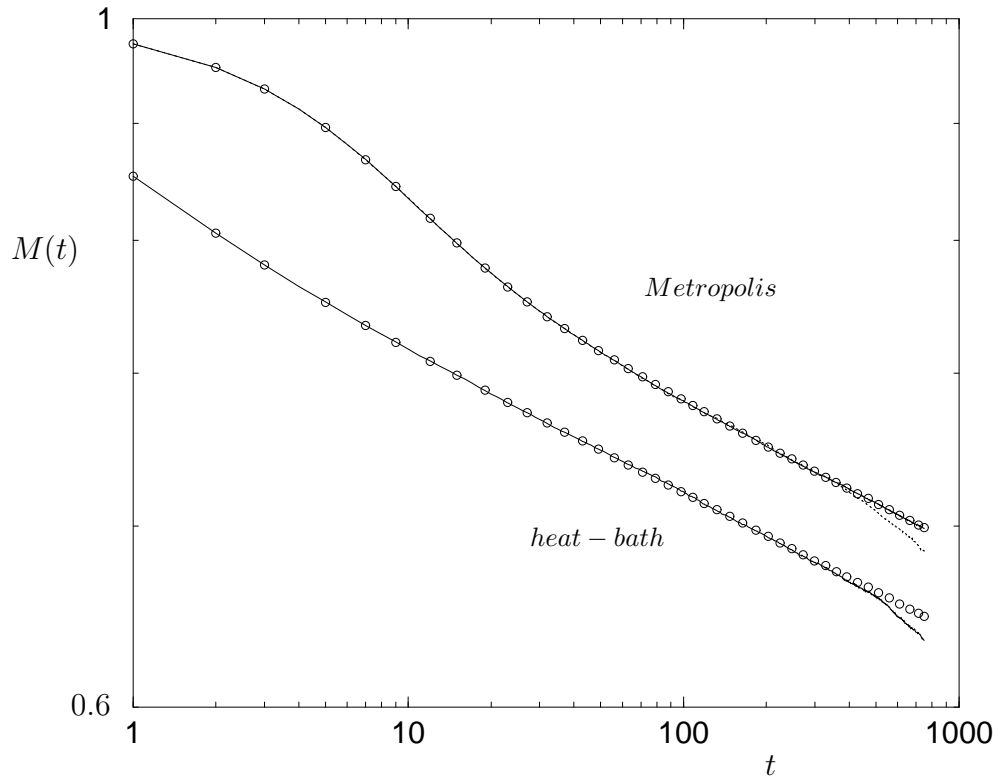


Figure 2: The time evolution of the magnetization for different lattice sizes and algorithms is plotted in double-log scale for the XY model. The upper branch of the curves is for the Metropolis algorithm while the lower one is for the heat-bath algorithm. The dotted lines, solid lines and circles correspond to the lattice size $L = 32, 64$ and 128 .

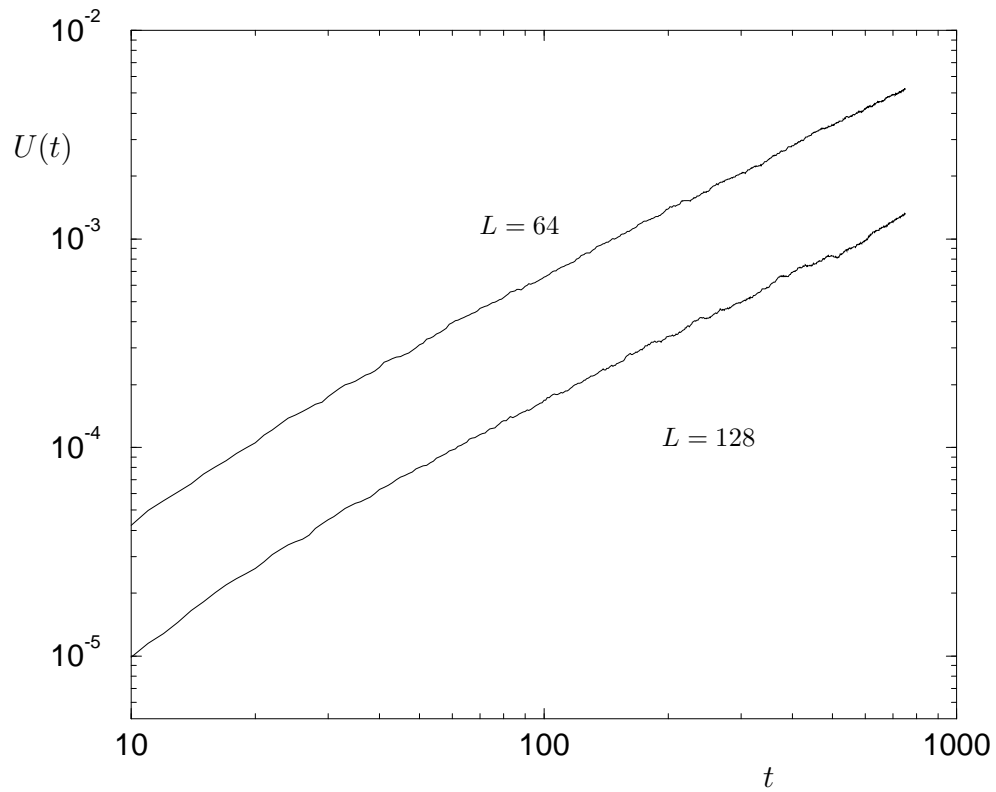


Figure 3: The time-dependent Binder cumulant for $L = 64$ and 128 with the Metropolis algorithm is plotted in double-log scale for the XY model.

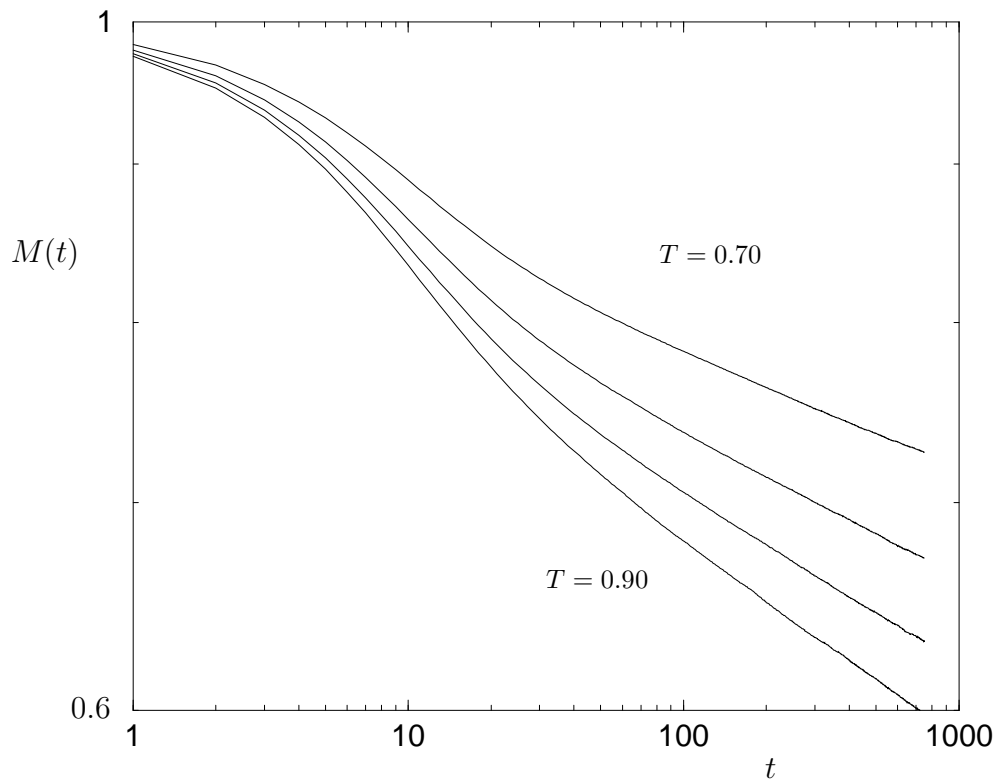


Figure 4: The time evolution of the magnetization for $L = 64$ with different temperatures is plotted in double-log scale for the XY model. The Metropolis algorithm is used in the simulations. From above, the temperature is $T = 0.70$, 0.80, 0.86 and 0.90 respectively.

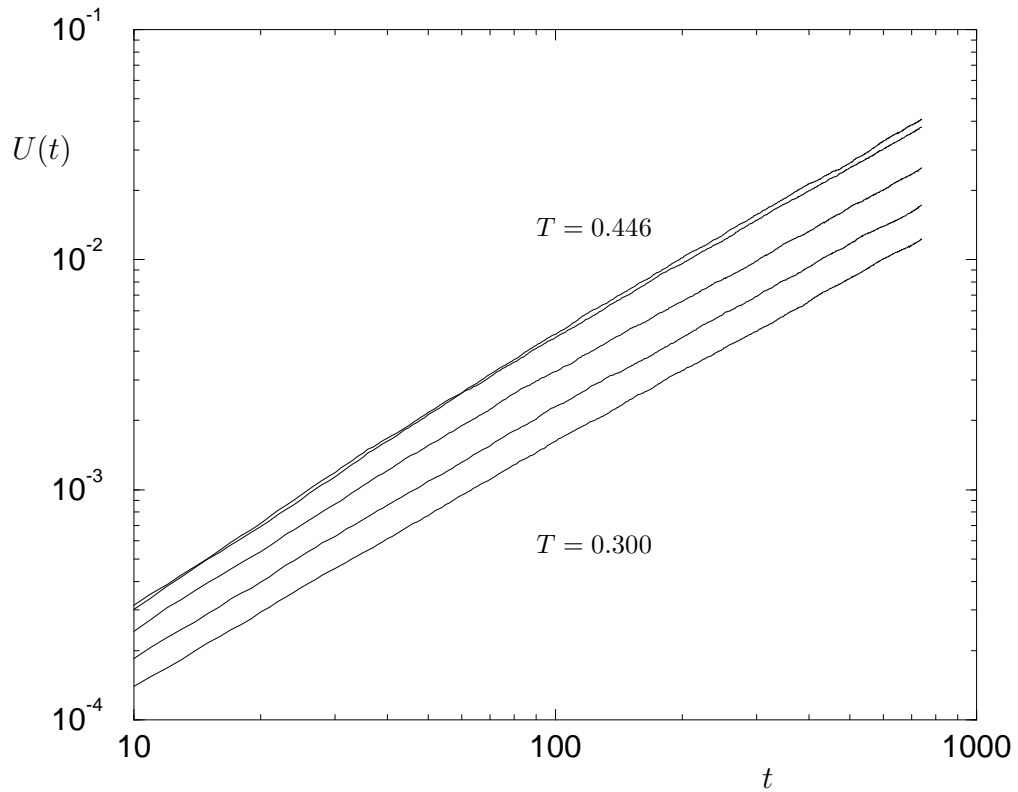


Figure 5: The time-dependent Binder cumulant for $L = 64$ with different temperatures is plotted in double-log scale for the FFXY model. The Metropolis algorithm is used in the simulations. From above, the temperature is $T = 0.446$, 0.440 , 0.400 , 0.350 and 0.300 respectively.